Zeitschrift: Helvetica Physica Acta

Band: 58 (1985)

Heft: 2-3

Artikel: Dynamics of commensurate and incommensurate vortex phases in a two-dimensional superconductor

Autor: Martinoli, P. / Beck, H. / Racine, G.A.

DOI: https://doi.org/10.5169/seals-115611

Nutzungsbedingungen

Die ETH-Bibliothek ist die Anbieterin der digitalisierten Zeitschriften auf E-Periodica. Sie besitzt keine Urheberrechte an den Zeitschriften und ist nicht verantwortlich für deren Inhalte. Die Rechte liegen in der Regel bei den Herausgebern beziehungsweise den externen Rechteinhabern. Das Veröffentlichen von Bildern in Print- und Online-Publikationen sowie auf Social Media-Kanälen oder Webseiten ist nur mit vorheriger Genehmigung der Rechteinhaber erlaubt. Mehr erfahren

Conditions d'utilisation

L'ETH Library est le fournisseur des revues numérisées. Elle ne détient aucun droit d'auteur sur les revues et n'est pas responsable de leur contenu. En règle générale, les droits sont détenus par les éditeurs ou les détenteurs de droits externes. La reproduction d'images dans des publications imprimées ou en ligne ainsi que sur des canaux de médias sociaux ou des sites web n'est autorisée qu'avec l'accord préalable des détenteurs des droits. En savoir plus

Terms of use

The ETH Library is the provider of the digitised journals. It does not own any copyrights to the journals and is not responsible for their content. The rights usually lie with the publishers or the external rights holders. Publishing images in print and online publications, as well as on social media channels or websites, is only permitted with the prior consent of the rights holders. Find out more

Download PDF: 30.11.2025

ETH-Bibliothek Zürich, E-Periodica, https://www.e-periodica.ch

Helvetica Physica Acta, Vol. 58 (1985) 427–442 0018–0238/85/020427–16$1.50 + 0.20/0
© Birkhäuser Verlag Basel, 1985

Dynamics of commensurate and incommensurate vortex phases in a two-dimensional superconductor

By P. Martinoli, H. Beck, G. A. Racine, F. Patthey and Ch. Leemann, Institut de Physique, Université de Neuchâtel, CH-2000 Neuchâtel, Switzerland

(19. X. 1984)

In honor of Emanuel Mooser's 60th birthday

Abstract. A study of the complex vortex response at radio-frequencies of superconducting films with periodically modulated thickness is reported. In this system, depending on vortex density and temperature, the two-dimensional vortex lattice undergoes a transition from a commensurate (C) phase in registry with the film periodicity to an incommensurate (I) phase. The CI-transition is triggered by soliton excitations which, at low temperature, form a one-dimensional superlattice in the I-phase. Structures emerging at well defined vortex densities in both the real and imaginary parts of the rf vortex response are interpreted as a signature of the CI-transition. A theoretical calculation of the vortex response based on the dynamics of an elastic dissipative vortex continum with discommensurations provides a good qualitative description of the rf-signals observed at low temperatures. It is shown that the mechanism responsible for the occurrence of the structures at the CI-transition is the break of translational symmetry caused by the formation of the soliton superlattice.

I. Introduction

Modulated structures whose period is incommensurable with that of the underlying lattice have been discovered and studied in a variety of condensed-matter systems [1]. They are usually observed in systems showing two competing periodicities as, for instance, rare-gas monolayers adsorbed at the surface of a solid, crystals with two interpenetrating incommensurate sublattices, metallic conductors undergoing a Peierls transition leading to the formation of a charge density wave and helical or sinusoidal magnetic structures incommensurable with the crystal lattice in certain rare-earth compounds. Moreover, the very existence of commensurate (C) and incommensurate (I) phases has also been demonstrated for a two-dimensional (2D) lattice of vortices in thin superconducting films whose thickness is periodically modulated in one direction [2–7]. In this paper we show how some of the features characterizing the CI-phase transition of the 2D vortex crystal in modulated layers can be seen in a study of the dynamic response of the vortices to a small rf driving field.

The phase diagram of 2D crystals exposed to a periodic 1D force field has been studied by Pokrovsky and Talapov [8] and by Martinoli et al. [7]. At low temperatures, where melting phenomena driven by the unbinding of thermally excited dislocation pairs [9–11] are expected to be irrelevant, it is determined by considering only one particular type of topological excitations, called solitons (or

discommensurations), which trigger the instability of a C-phase with respect to an I-phase. The I-phase is characterized by a 1D soliton superlattice, of period P, varying, for the incompressible lattice of vortices, under an angle 45° with respect to $\vec{q}_0$, the wave vector of the 1D thickness modulation. For an infinite 2D vortex crystal at $T=0$ a CI-phase transition, at which P diverges, occurs whenever the deviations from a configuration $\vec{q}_0=\vec{g}_{mn}$ corresponding to perfect matching ($\vec{g}_{mn}$ is a reciprocal vortex lattice vector) are such that the mismatch parameter $\delta=1-(g_{mn}/q_0)$ reaches the critical value $\delta_c=(2/\pi)(\Delta/\mu)^{1/2}$, where Δ is the amplitude of the cosine pinning potential and μ the shear modulus [12] of the vortex lattice.

To study the dynamic response of the pinned vortex medium, we rely on a modified version of the two-coil technique devised by Fiory and Hebard [13]. With the vortex crystal in a C-phase, this method does not excite transverse modes of an infinite lattice. In such a phase coupling to lattice shear modes only arises from the finite size of the sample, from Umklapp (U)-processes and/or from residual random pinning. In a I-phase, on the other hand, the 1D periodic sequence of solitons breaks the translational symmetry of the vortex lattice, thereby allowing intrinsic coupling of the oscillating driving field to transverse modes of the soliton superlattice. Thus, pronounced structures reflecting the occurrence of the CI-phase transition at $\delta=\delta_c$ are expected in the rf complex vortex response of thickness modulated layers as the transverse magnetic field B (and, consequently, δ) is swept across the value, B_{mn}, defining a configuration of perfect matching ($\delta=0$) [5, 7]. The detection of these structures (Section II) as well as their theoretical interpretation (Section IV) in terms of a model for the dynamics of the 2D vortex medium in its different phases (Section III) are the central object of the present paper.

II. Experimental results

The experiments were performed on a thickness modulated ($\lambda_0=2\pi/q_0=0.73\ \mu$m) granular Al-film [2, 7] with a BCS-transition temperature, T_c, of 2.05 K, a normal-state sheet resistance, $R_{n\square}$, of 25 Ω, an average thickness, d, of 500 Å and a relative thickness modulation, $\Delta d/d$, of the order of 10%. As shown in Fig. 1, excitation of the vortex medium was provided by two elongated rectangular (20 mm × 1.8 mm) coils, D_1 and D_2, placed at an average height, h_D, of approximately 0.5 mm above the film surface and driven in opposition by a 5 μA rf-current, I_a, of angular frequency ω. With this coil configuration, the driving 'Meissner' sheet supercurrent density $\vec{J}_M$ flowing in that region of the film, located between D_1 and D_2, which significantly contributes to the rf-voltage detected by the receive coil R (Fig. 1) is nearly unidirectional and parallel to the unit vector $\hat{D}$ shown in Fig. 1. The square-shaped (4 mm × 4 mm) receive coil R lies in a plane perpendicular to the superconducting layer, the distance, h_R, of closest approach of its winding to the film surface being of the order of 0.1 mm. The rf-signal, which was phase-sensitively detected against rf-drive, contains two contributions. The first one, denoted by V, arises from the total sheet current density $\vec{J}$ flowing in the modulated film. $\vec{J}$ is the sum of $\vec{J}_M$ and of the 'vortex' sheet current density $\vec{J}_v$ resulting from the oscillating motion of the vortices driven by $\vec{J}_M$ [14]. The second one is the pick-up signal at R due to the rf-current circulating in D_1 and

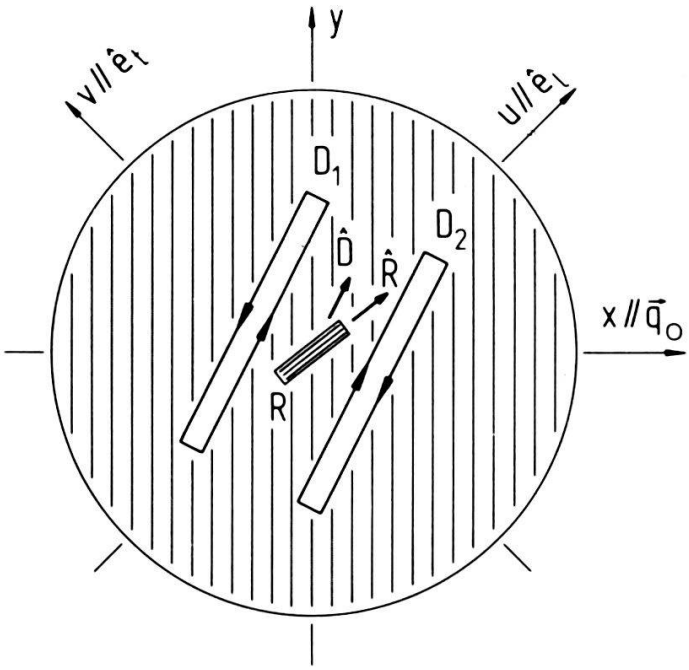

Figure 1
Geometry of the drive (D_1 and D_2)–receive (R) coil configuration used to measure the rf-response of commensurate and incommensurate vortex phases in a thickness-modulated superconducting film.

D_2. In order to discriminate the genuine film response V against the spurious film-independent pick-up, a low-frequency ($\sim$3 Hz) weak-field ($\Delta B \sim 0.1$ gauss) modulation technique was used. As a result, the actually detected signal at R turns out to be proportional to $\partial V/\partial B$. Moreover, to study the angular dependence of the rf-response, the orientation of the R-coil relative to D_1 and D_2, as determined by the unit vectors $\hat{R}$ and $\hat{D}$ in Fig. 1, was changed and the whole coil arrangement was rigidly rotated with respect to $\vec{q}_0$, which is assumed to be parallel to the x-axis. We shall denote by (α, β) a coil configuration such that the driving force on the vortices, $\vec{F}_L = (\phi_0/c)(\vec{J}_M \times \hat{z})$, provided by D_1 and D_2 is in the α-direction while the orientation of the R-coil is such that it detects the response arising from the projection of vortex motion along the β-direction.

Data taken at 3 MHz and at different temperatures are shown in Fig. 2 for the (y, y)-coil configuration. Pronounced structures in both the in-phase and out-of-phase components of $\partial V/\partial B$ emerge from a monotonically varying background around $B_{10} = (\sqrt{3}/2)(\phi_0/\lambda_0^2) = 33.6$ gauss, the field defining the fundamental matching configuration ($m = 1$, $n = 0$) [5–7]. These structures, which are not resolved at low temperatures ($T < 1.7$ K), show up at about 1.7 K and, after an initial growth in strength with increasing temperature, gradually disappear at higher temperatures. It should also be noticed that, although comparable in magnitude, the imaginary part of the signal around B_{10} is systematically larger than its real part. Even though not so well-resolved as those shown in Fig. 2, structures reflecting the CI-phase transition of the 2D vortex lattice were observed also in the vicinity of B_{11} and B_{20}, the fields corresponding to higher-order matching configurations.

Signals corresponding to the (x, x)-coil configuration are shown in Fig. 3. While similar in shape and magnitude to those of the (y, y)-configuration at low temperatures [curve (d)], these structures are quite different from those shown in Fig. 2 at high temperatures [curve (a)]. A striking feature emerging from these

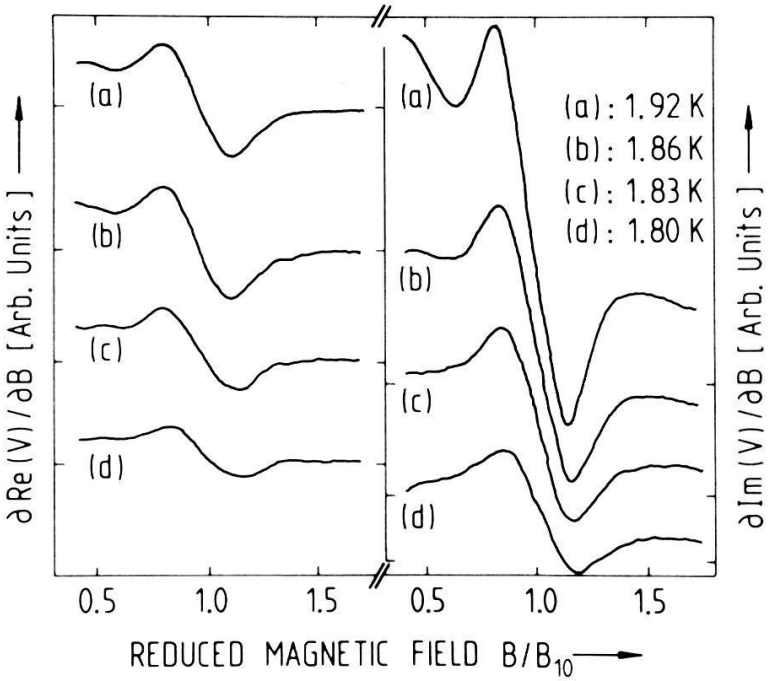

Figure 2
Magnetic field dependence of the complex vortex response of a thickness-modulated Al-film measured at 3 MHz with the (y, y)-coil configuration. Marks on the vertical axis denote the zero-level of the signals.

data is the appearance, as T progressively rises, of a new signal which washes out almost completely the (weak) structure assigned to the low-temperature CI-transition in the real component and generates additional structure in the imaginary part of $\partial V/\partial B$. The strong anisotropic character of the high-temperature signals shows up quite clearly as the coils are progressively rotated form the (y, y)-towards the (x, x)-configuration. While at low temperatures only minor

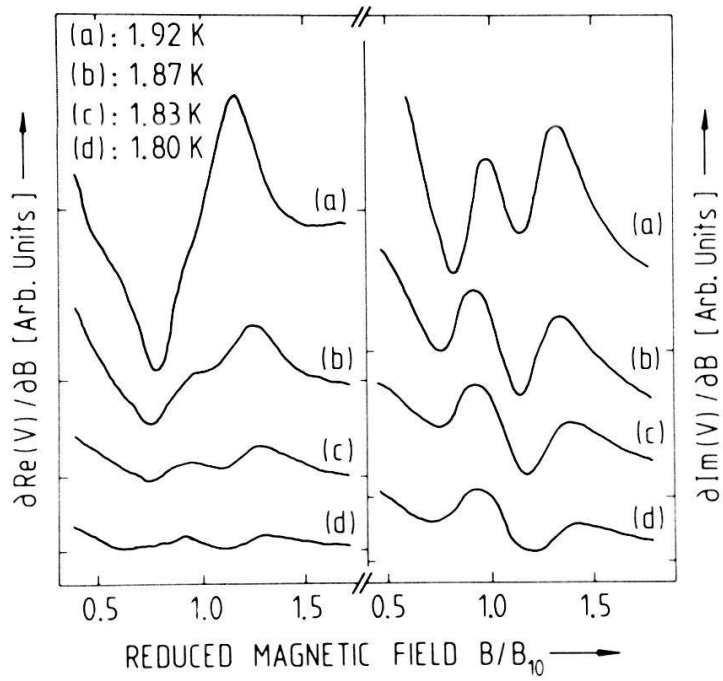

Figure 3
As Fig. 2, but for the (x, x)-coil configuration.

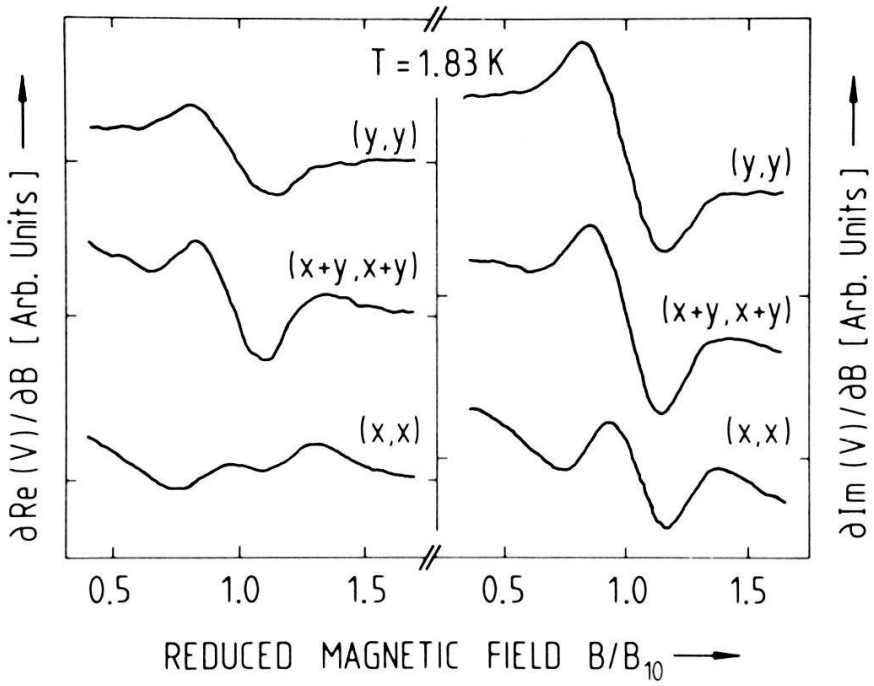

Figure 4
Magnetic field dependence of the low-temperature complex vortex response at 3 MHz for three different coil configurations. The film is the same as in Fig. 2.

changes in the shape of the structures are observed (Fig. 4), profound modifications in the form of both components of $\partial V/\partial B$ occur at higher temperatures (Fig. 5). Although the origin of the additional feature observed when the measuring coils are in the (x, x)-configuration might well be related to the CI-phase transition of the 2D vortex crystal, the fact that it only shows up at high temperatures indicates that it cannot be associated with the type of low-temperature CI-transition described in this paper.

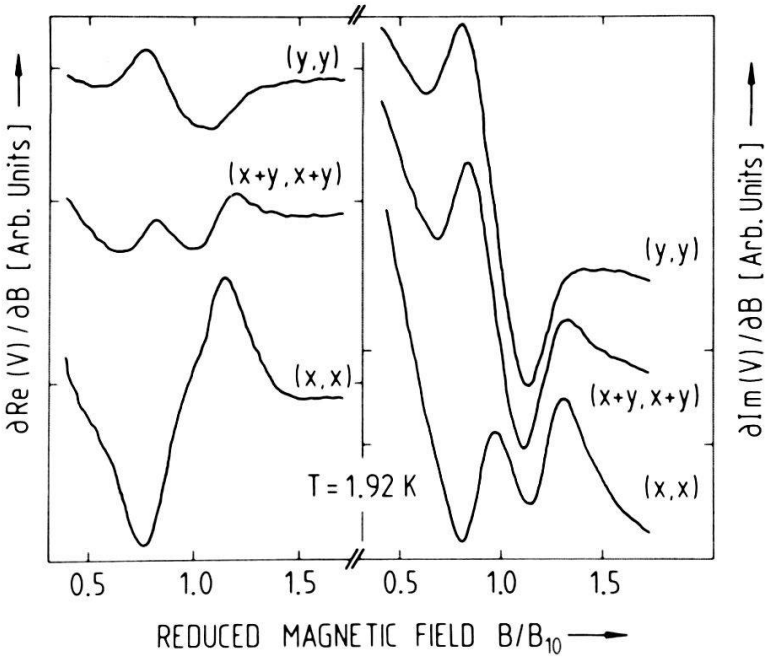

Figure 5
As Fig. 4, but at a higher temperature.

III. Vortex dynamics

To study the dynamics of the vortex lattice in its various phases, we shall focus our attention on situations where $\vec{q}_0$ is close to one of the reciprocal vortex lattice vectors $\vec{g}_{mn}$. Furthermore, it is assumed that the periodic pinning potential is weak when compared to the lattice stiffness, i.e. $\Delta < \mu$. Under this condition the triangular vortex lattice can be treated as an isotropic 2D elastic continuum with Lamé coefficients λ and μ [15]. Then, the equation of motion for the deformation field $\vec{w}$ of the dissipative 2D vortex medium driven by the oscillating force $\vec{F}_L = (B/c)(\vec{J}_M \times \hat{z})$ in the periodic potential $U(\phi)$, where $\phi = w_x + \delta x$ is the displacement of the vortices, in the x-direction (Fig. 1), with respect to the bottom of the corresponding potential wells, can be written in the form [15]:

$$\eta \frac{\partial \vec{w}}{\partial t} = \mu \nabla^2 \vec{w} + (\lambda + \mu) \nabla \nabla \cdot \vec{w} - \nabla_\phi U + \vec{F}_L, \tag{1}$$

where $\eta = B^2/c^2 R_\square$ is the viscosity coefficient [16] expressed in terms of the sheet flux-flow resistance $R_\square$. Since we are interested in the linear dynamic response of the vortex lattice to the driving force $\vec{F}_L$, it is convenient to write $\vec{w}$ in the form $\vec{w} = \vec{w}_e + \vec{s}$ and to expand equation (1) to first order in the deviation $\vec{s}$ from the static (equilibrium) deformation field $\vec{w}_e$. As shown in Ref. 7, for an infinite 2D vortex crystal $\vec{w}_e$ consists in a homogeneous area-conserving deformation in a C-phase onto which a 1D soliton lattice is superposed in an I-phase. In Section III(C) we shall show how the finite size of the sample can be accounted for by allowing for the nucleation of boundary solitons in a C-phase [17]. Linearizing equation (1) in the small dynamic displacement $\vec{s}$ one obtains the following equation for vortex motion:

$$\eta \frac{\partial \vec{s}}{\partial t} + \hat{\mathbb{L}} \vec{s} = \vec{F}_L, \tag{2}$$

where $\hat{\mathbb{L}}$ is a 2×2 matrix operator whose components are given by:

$$\hat{\mathbb{L}}_{\alpha\beta} = -\mu \nabla^2 \delta_{\alpha\beta} - (\lambda + \mu) \nabla_\alpha \nabla_\beta + \hat{q}_{0\alpha} U''(\phi_e) \hat{q}_{0\beta} \tag{3}$$

with $\phi_e = w_{ex} + \delta x$. Equation (2) is a linear inhomogeneous partial differential equation, whose solutions $\vec{s}(\vec{r}, t)$ can be expressed in terms of the normalized eigenvectors $\vec{\Phi}_{\mathbf{K}}$ and of the eigenvalues $E(\vec{K})$ of the operator $\hat{\mathbb{L}}$:

$$\hat{\mathbb{L}} \vec{\Phi}_{\mathbf{K}} = E(\vec{K}) \vec{\Phi}_{\mathbf{K}}. \tag{4}$$

Taking an $e^{i\omega t}$-time dependence for $\vec{F}_L$, the ω-Fourier component, $\vec{s}_\omega(\vec{r})$, of $\vec{s}(\vec{r}, t)$ can be written as:

$$\vec{s}_\omega(\vec{r}) = \sum_{\mathbf{K}} \frac{\langle \Phi_{\mathbf{K}} \mid F_{L\omega} \rangle}{i\eta\omega + E(\vec{K})} \vec{\Phi}_{\mathbf{K}}(\vec{r}), \tag{5}$$

where the scalar product is defined by:

$$\langle f \mid g \rangle = \frac{1}{L^2} \int (\vec{f}^* \cdot \vec{g}) d^2 r, \tag{6}$$

L being the (linear) size of the sample, which is assumed to have a square shape.

At this stage the problem is reduced to that of finding the eigenvectors $\vec{\Phi}_{\mathbf{K}}$ and eigenvalues $E(\vec{K})$ of the operator $\hat{\mathbb{L}}$ in the different phases assumed by the vortex lattice. For the sake of simplicity, in the mathematical calculations it is convenient to choose, instead of a cosine potential, a piece-wise parabolic periodic potential such that $U(\phi_e) = (1/2)\kappa\phi_e^2$ in the interval $-(\lambda_0/2) \leq \phi_e \leq (\lambda_0/2)$.

A. *The commensurate* (C) *phase* ($\delta < \delta_c$)

In the ground state of an infinite 2D vortex crystal in a C-phase ($\delta < \delta_c$) each vortex of the lattice lies at the bottom of a potential well, i.e. $\phi_e \equiv 0$ everywhere [7]. As a consequence, the curvature $U''(\phi_e)$ of the periodic potential experienced by the vortices, which appears in the last term of equation (3), is a constant which takes the value κ for our particular choice of $U(\phi_e)$. Then, for an incompressible ($\lambda \to \infty$) lattice of vortices the solutions of equation (4) are plane waves of the form:

$$\vec{\Phi}_{\mathbf{K}}(\vec{r}) = \hat{e}_t(\vec{K})e^{i\vec{K}\cdot\vec{r}}, \tag{7}$$

where $\hat{e}_t(\vec{K})$ is a polarization vector for transverse lattice deformation modes $[\hat{e}_t(\vec{K}) \cdot \vec{K} = 0]$ and the wave vector $\vec{K}$ is confined within the first Brillouin zone. The corresponding eigenvalues are given by:

$$E(\vec{K}) = \mu K^2 + \kappa \frac{K_y^2}{K^2}, \tag{8}$$

where K_y is the component of $\vec{K}$ along the y-direction, perpendicular to $\vec{q}_0$, shown in Fig. 1. As expected, for vortex motion perpendicular to the grooves of the periodic potential, i.e. for shear modes such that $\vec{K} \cdot \vec{q}_0 = 0$, there is a gap, of value κ, in the dispersion relation (8) at $K = 0$.

B. *The incommensurate* (I) *phase* ($\delta > \delta_c$)

The 1D soliton superlattice, which characterizes the ground state of the 2D vortex crystal in the I-phase ($\delta > \delta_c$), is described by the 'phase' field ϕ_e, a stair-shaped function [7] varying only along a direction u which, for the incompressible vortex lattice, is found to form an angle of 45° with the x-axis (Fig. 1). Since ϕ_e only depends on u and is such that $\phi_e(u + nP) = \phi_e(u) + n\lambda_0$, the last term of equation (3), which contains the curvature $U''(\phi_e)$, is a periodic function of u with period P: $U''[\phi_e(u + nP)] = U''[\phi_e(u)]$. Anticipating external forces $\vec{F}_L$ which are almost spatially homogeneous (see Section IV), this suggests to look for solutions of equation (4) varying only along the u-direction, i.e. of the form $\vec{\Phi}_{\mathbf{K}} = \vec{\Phi}_{\mathbf{K}}(u)$. It is then easily seen that, in the $u - v$ reference frame of Fig. 1, equation (4) takes the form of a (1D) matrix Schrödinger equation for the 'spinor' field $\vec{\Phi}_{\mathbf{K}}(u)$ describing the motion of a particle in the 1D periodic potential $U''[\phi_e(u)]$. As a consequence, $\vec{\Phi}_{\mathbf{K}}(u)$ is a Bloch function of the form:

$$\vec{\Phi}_{\mathbf{K}}(u) = \vec{\Psi}_{\mathbf{K}}(u)e^{iKu}, \tag{9}$$

where $\vec{\Psi}_{\mathbf{K}}(u)$ is such that $\vec{\Psi}_{\mathbf{K}}(u + nP) = \vec{\Psi}_{\mathbf{K}}(u)$ and the Bloch wave vector $\vec{K}$ is parallel to the u-direction. To find an explicit form of the eigenfunctions $\vec{\Phi}_{\mathbf{K}}(u)$, we rely on our particular choice for $U(\phi_e)$. In this case the static soliton solution

$\phi_e(u)$, in the limit $\lambda \to \infty$, is given by [18]:

$$\phi_e(u) = \frac{\lambda_0}{2} \sum_n \chi(u - nP) \left[\frac{\sinh \varepsilon(u - nP)}{\sinh(\varepsilon P/2)} + 2n \right], \tag{10}$$

where $\chi(z)$ is such that $\chi(z) = 1$ for $-(P/2) \leq z \leq (P/2)$ and vanishes otherwise and $\varepsilon^2 = \kappa/2\mu$. The period P is related to the mismatch parameter δ and, consequently, to the magnetic field B by [18]:

$$\frac{\delta}{\delta_c} = \coth(\varepsilon P/2) + \frac{(\varepsilon P/2)}{\sinh^2(\varepsilon P/2)}, \tag{11}$$

where $\delta_c = \varepsilon\lambda_0/4\sqrt{2}$. With $\phi_e(u)$ given by equation (10) one can easily show that $U''[\phi_e(u)]$ yields a Kronig-Penney potential of the form:

$$U''[\phi_e(u)] = \kappa - \frac{2\kappa}{\varepsilon} \tanh(\varepsilon P/2) \sum_n \delta(u - nP). \tag{12}$$

Since $U''[\phi_e(u)] = \kappa$ between the (negative) 'spikes' of the periodic potential (12), we look, in these regions, for solutions of the form:

$$\vec{\Phi}_{\mathbf{K}}(u) = \vec{a}_{\mathbf{K}} e^{ik_{\mathbf{K}}u} + \vec{b}_{\mathbf{K}} e^{-ik_{\mathbf{K}}u} \tag{13}$$

which, after substitution in equation (4), lead to the following expression for $E(\vec{K})$:

$$E(\vec{K}) = \tfrac{1}{2}(\kappa + 2\mu k_{\mathbf{K}}^2). \tag{14}$$

Relying on Bloch's theorem, which requires that $\vec{\Phi}_{\mathbf{K}}(u + P) = e^{iKP}\, \vec{\Phi}_{\mathbf{K}}(u)$, one can match at a 'spike' solutions corresponding to successive regions by imposing continuity as in quantum mechanics [19]. For an incompressible lattice this procedure leads to the following condition for $k_{\mathbf{K}}$:

$$\cos KP = \cos(k_{\mathbf{K}} P) - \varepsilon P \tanh(\varepsilon P/2) \frac{\sin(k_{\mathbf{K}} P)}{k_{\mathbf{K}} P}. \tag{15}$$

The dispersion relation $E(\vec{K})$ resulting from equations (14) and (15) is shown in Fig. 6, where the 'acoustical' branch located betwen $-\pi/P$ and $+\pi/P$ corresponds to the so-called phason mode [20] of the soliton lattice.

It will be shown in Section IV that the relevant Bloch wave vectors $\vec{K}$ of our experiments are the non-vanishing reciprocal vectors $\vec{G}$ of the 1D soliton superlattice $[G = n(2\pi/P)]$. In this particular case and for the incompressible vortex lattice $\vec{\Phi}_{\mathbf{G}}(u)$ takes the simple form:

$$\vec{\Phi}_{\mathbf{G}}(u) = A\hat{e}_t(\vec{K}) \cos k_{\mathbf{G}}\left(u - \frac{P}{2}\right), \tag{16}$$

where $\hat{e}_t(\vec{K})$ is a polarization vector for transverse excitation modes of the 1D soliton lattice, i.e. $\hat{e}_t(\vec{K}) \cdot \vec{K} = 0$ with $\vec{K}$ parallel to the u-axis (see Fig. 1), and $k_{\mathbf{G}}$ is one (still unspecified) solution of equation (15) for $\vec{K} = \vec{G}$ (see Section IV for a discussion of this point). The amplitude A is determined by the condition $\langle \Phi_{\mathbf{K}} \mid \Phi_{\mathbf{K}'} \rangle = \delta_{\mathbf{K}\mathbf{K}'}$:

$$A^2 = 2\left[1 + \frac{\sin(k_{\mathbf{G}} P)}{k_{\mathbf{G}} P}\right]^{-1}. \tag{17}$$

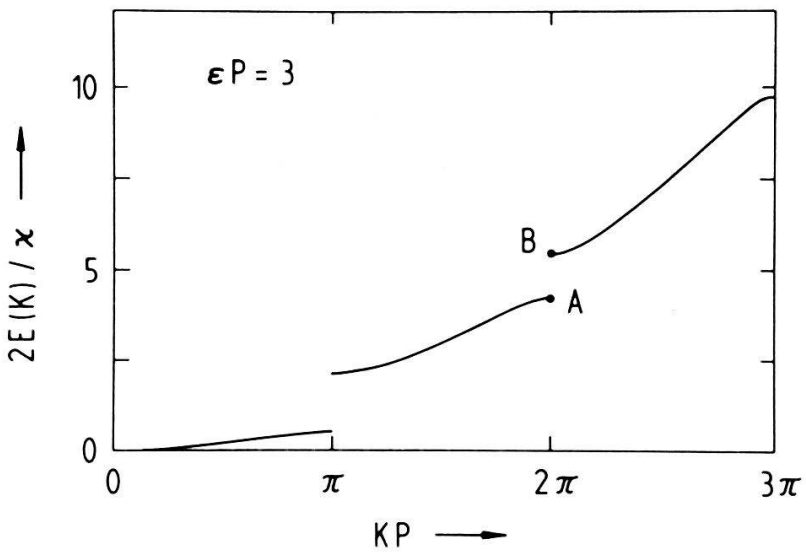

Figure 6
Dispersion relation for the soliton lattice of an incommensurate vortex phase. Only even standing waves, corresponding to points like A, contribute to the vortex response measured in our experiments.

C. *Size effects*

For a sample of finite size one should allow for the nucleation of soliton-like topological excitations at the edges (boundary solitons) when the bulk of the vortex lattice is in a C-phase [17]. The situation is schematically illustrated by Fig. 7, where, for the sake of simplicity, we have assumed that the orientation of our square sample is such that its edges form an angle of ±45° with the x-axis. Then, boundary solitons will form at two opposite edges of the sample. As shown by Fig. 7(a), for $P(\delta) < L$ the vortex lattice is in the I-phase. It is assumed that in this case edge effects have negligible influence on the vortex dynamics, so that the calculations for the infinite incommensurate crystal of Section III(B) still apply as long as $P(\delta) < L$. For $\delta < \delta_0$, where δ_0 is such that $P(\delta_0) = L$, soliton nucleation is possible only at two opposite boundaries of the sample, the bulk of the vortex lattice being in a C-phase. For $\delta = \delta_0$ [Fig. 7(b)], i.e. $P(\delta_0) = L$, one single soliton, having precisely the same features as those studied in the previous subsection, exactly fits into the sample. Thus, its amplitude at the edges, as deduced from equation (10), is $\phi_e(L/2) = -\phi_e(-L/2) = \lambda_0/2$. For $P(\delta) > L$, i.e. $\delta < \delta_0$, the size L is too small for the system to be able to accommodate a 'complete' soliton, i.e. a soliton for which the 'phase' jump $\phi_e(L/2) - \phi_e(-L/2)$ amounts to λ_0. As a consequence, the soliton amplitude at the edges decreases as δ is progressively reduced below δ_0 and finally vanishes for $\delta = 0$ [Fig. 7(c)]. An obvious phenomenological way to take into account this effect is to write the soliton amplitude at the boundaries as $\phi_e(L/2) = -\phi_e(-L/2) = (\lambda_0/2)(\delta/\delta_0)^\gamma$, where the (positive) exponent γ turns out to be equal to 1 if one applies the result of Ref. 17 to our piece-wise parabolic potential. To study the dynamics of superconducting vortices in a C-phase with boundary solitons [$P(\delta) > L$], it is convenient to impose again periodic boundary conditions to equation (4) by requiring that $\vec{\Phi}_{\mathbf{K}}(u + L) = e^{iKL}\vec{\Phi}_{\mathbf{K}}(u)$. The problem is then formally identical to that solved in Section III(B), the (fixed) periodicity, however, being now L rather than $P(\delta)$. For our particular choice of $U(\phi_e)$ the above expression for the soliton amplitude at the boundaries

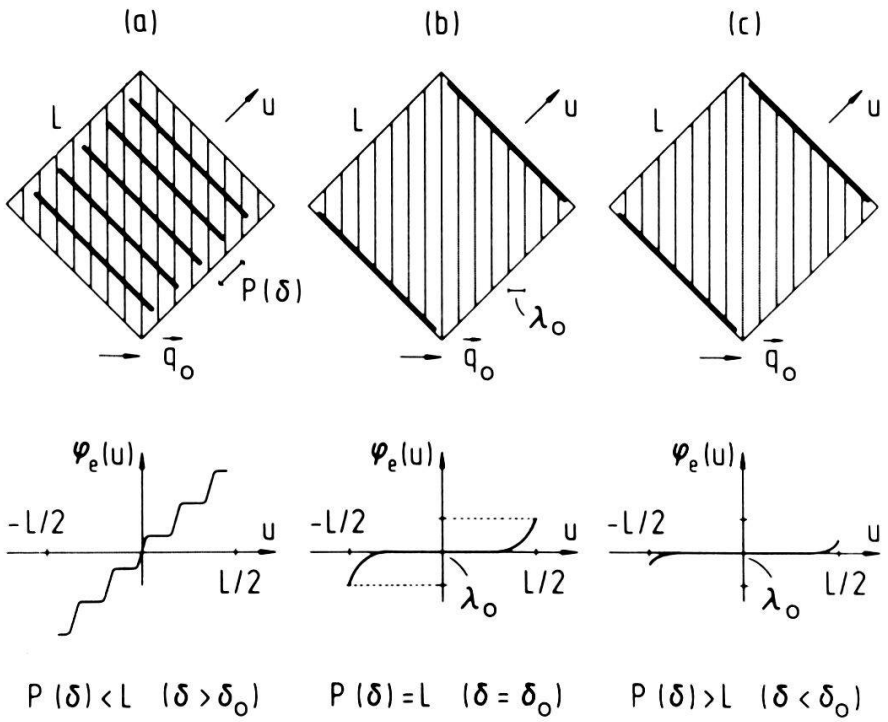

Figure 7
Solitons in a sample of finite size: (a) Incommensurate (striped) phase; (b) Commensurate phase showing boundary solitons with full amplitude at the edges; (c) Commensurate phase with boundary solitons of reduced edge amplitude.

suggests a Kronig-Penney potential of the form (for $\delta < \delta_0$):

$$U''[\phi_e(u)] = \kappa - \frac{2\kappa}{\varepsilon}(\delta/\delta_0)^\gamma \tanh(\varepsilon L/2) \sum_n \delta(u - nL). \tag{18}$$

From equation (12), which is valid for $P(\delta) \leqslant L$ ($\delta \geqslant \delta_0$), and equation (18), which applies for $P(\delta) \geqslant L$ ($\delta \leqslant \delta_0$), it is seen that the I-phase and the C-phase with boundary solitons are correctly matched at $\delta = \delta_0$, where $P(\delta_0) = L$. It is also clear that, with $U''[\phi_e(u)]$ given by equation (18), equations (14)–(17) of the previous subsection still apply when $P(\delta) > L$ with the prescription, however, of replacing P by L everywhere and with an additional factor $(\delta/\delta_0)^\gamma$ in the last term of equation (15).

What is the appropriate size L in real films? To answer this nontrivial question, we notice that the granular structure of the modulated Al-films used in our experiments represents a dense system of randomly distributed weak pinning centers acting on the vortices. Under these circumstances long-range positional order no longer exists in the vortex medium. An almost periodic vortex lattice only occurs within domains whose size is determined by the Larkin-Ovchinnikov correlation length R_c [21], which is typically of the order of 10–50 lattice constants [22]. Therefore, we expect the appropriate L for our films to be approximately of the order of R_c and, consequently, much smaller than the actual sample size.

IV. The rf vortex response

Relying on the vortex dynamics studied in the previous Section, we shall now derive a theoretical expression for the rf-signal V generated in the receive coil R

by the sheet current density $\vec{J}(\vec{r}, t) = \vec{J}_M(\vec{r}, t) + \vec{J}_v(\vec{r}, t)$ flowing in a thickness-modulated film in response to the rf-excitation provided by the drive coils D_1 and D_2 (see Section II and Fig. 1).

We consider a very thin superconducting film, such that $d \ll \lambda$, where λ is the temperature dependent penetration depth. Under this condition, the superconducting layer is truly two-dimensional and can be thought of as being confined to a plane which, for convenience, is assumed to be the $z = 0$-plane. The 'usual' current density $\vec{j}(\vec{r}, z, t)$ is then related to the 'sheet' current density $\vec{J}(\vec{r}, t)$ simply by $\vec{j} = \delta(z)\vec{J}$. To calculate the rf-response V, we consider the vector potential variation $\overrightarrow{\delta A}(\vec{r}, z, t) = \vec{A}(\vec{r}, z, t) - \vec{A}_a(\vec{r}, z, t)$ due to $\vec{J}(\vec{r}, t)$, $\vec{A}$ and $\vec{A}_a$ being, respectively, the (total) vector potential generated by $\vec{J}$ and $\vec{j}_a$ (the current density associated with the rf-current I_a circulating in D_1 and D_2) and the vector potential created by $\vec{j}_a$ alone. Then, if the driving frequency, $\omega/2\pi$, is not too high, $\vec{A}(\vec{r}, z, t)$ satisfies, in all space, Maxwell's equation:

$$\nabla \times \nabla \times \vec{A} = \frac{4\pi}{c}[\delta(z)\vec{J} + \vec{j}_a], \tag{19}$$

while, within the 2D superconducting film, $\vec{J}$ obeys London's equation [23]:

$$\vec{J} = \frac{c}{2\pi\Lambda}(\vec{\Phi} - \vec{A}), \tag{20}$$

where $\Lambda = 2\lambda^2/d$ is the effective penetration depth for 2D superconductors. The 2D 'fluxoid' field $\vec{\Phi}(\vec{r}, t)$ describes vortex excitations at $\vec{r} = \vec{r}_j(t)$ and satisfies the equation [23]:

$$\nabla \times \vec{\Phi} = \phi_0 \sum_j \delta(\vec{r} - \vec{r}_j). \tag{21}$$

By means of the Fourier-transform method first applied by Pearl [23] to a similar problem, equations (19) and (20) can be solved for the $\vec{q}$-Fourier component, $\underset{\sim}{\overrightarrow{\delta A}}(\vec{q}, z, t)$, of $\overrightarrow{\delta A}(\vec{r}, z, t)$ giving:

$$\underset{\sim}{\overrightarrow{\delta A}}(\vec{q}, z, t) = [\underset{\sim}{\vec{\Phi}}(\vec{q}, t) - \underset{\sim}{\vec{A}}_a(\vec{q}, 0, t)]\frac{e^{-q|z|}}{1 + q\Lambda}, \tag{22}$$

where $\underset{\sim}{\vec{A}}_a(\vec{q}, 0, t)$ is related to $\underset{\sim}{\vec{j}}_a(\vec{q}, q_z, t)$, the 3D Fourier transform of $\vec{j}_a(\vec{r}, z, t)$, by [23]:

$$\underset{\sim}{\vec{A}}_a(\vec{q}, 0, t) = \frac{2\pi}{cq}\underset{\sim}{\vec{j}}_a(\vec{q}, q_z = -iq, t). \tag{23}$$

The Fourier component of the Meissner sheet current density is easily obtained from equations (19) and (20) by setting $\vec{\Phi} = 0$ [23]:

$$\underset{\sim}{\vec{J}}_M(\vec{q}, t) = -\frac{\underset{\sim}{\vec{j}}_a(\vec{q}, q_z = -iq, t)}{1 + q\Lambda}. \tag{24}$$

As it clearly results from equation (21), which contains the vortex positions $\{\vec{r}_j(t)\}$, the vortex dynamics enters the expresion (22) for $\underset{\sim}{\overrightarrow{\delta A}}(\vec{q}, z, t)$ through $\underset{\sim}{\vec{\Phi}}(\vec{q}, t)$ which is easily deduced from equation (21) if one notices that, as required by current continuity, $\nabla \cdot \vec{\Phi} = 0$:

$$\underset{\sim}{\vec{\Phi}}(\vec{q}, t) = i\phi_0 \frac{(\hat{q} \times \hat{z})}{q} \sum_j e^{-i\vec{q}\cdot\vec{r}_j(t)}. \tag{25}$$

Writing $\vec{r}_j(t)$ in the form $\vec{r}_j(t) = \vec{r}_{je} + \vec{s}(\vec{r}_{je}, t)$, equation (25) can now be linearized in the small oscillating displacement $\vec{s}(\vec{r}_{je}, t)$ of the vortex j about its static equilibrium position $\vec{r}_{je}$. Then, assuming again an $e^{i\omega t}$-time dependence for all fields and combining equations (22)–(25), the $(\vec{q}, \omega)$-Fourier component, $\underset{\sim}{\overrightarrow{\delta E}}_\omega(\vec{q}, z) = -(i\omega/c)\,\underset{\sim}{\overrightarrow{\delta A}}_\omega(\vec{q}, z)$, of the electric field $\overrightarrow{\delta E}(\vec{r}, z, t)$ generated by $\vec{J}(\vec{r}, t)$ can be written in the form:

$$\underset{\sim}{\delta E}_{\omega\alpha}(\vec{q}, z) = -\frac{e^{-q|z|}}{1+q\Lambda}\left[\sum_{q',\beta} R_{\omega\alpha\beta}(\vec{q}', \vec{q})\underset{\sim}{J}_{M\omega\beta}(\vec{q}') + i\omega L_K \frac{1+q\Lambda}{q\Lambda}\underset{\sim}{J}_{M\omega\alpha}(\vec{q})\right], \quad (26)$$

where $L_K = 2\pi\Lambda/c^2$ is the sheet kinetic inductance. The first term on the right-hand side of equation (26) is the contribution to $\underset{\sim}{\overrightarrow{\delta E}}_\omega(\vec{q}, z)$ due to the oscillating motion of the vertices. Thus, $R_{\omega\alpha\beta}(\vec{q}', \vec{q})$ is the 'vortex response function' in which we are primarily interested here. Using equation (5) for $\vec{s}_\omega(\vec{r}_{je})$ in the linearized equation for $\underset{\sim}{\vec{\Phi}}_\omega(\vec{q})$, it is readily shown that:

$$R_{\omega\alpha\beta}(\vec{q}', \vec{q}) = (\hat{q}\times\hat{z})_\alpha \frac{R_\square}{N^2}\sum_j e^{-i\vec{q}\cdot\vec{r}_{je}} \sum_{\mathbf{K}} \frac{i\omega\tau(\vec{K})}{1+i\omega\tau(\vec{K})}[\hat{q}\cdot\vec{\Phi}_{\mathbf{K}}(\vec{r}_{je})]$$
$$\times \sum_l e^{i\vec{q}'\cdot\vec{r}_{le}}[\hat{z}\times\vec{\Phi}^*_{\mathbf{K}}(\vec{r}_{le})]_\beta, \quad (27)$$

where $\tau(\vec{K}) = \eta/E(\vec{K})$ is the relaxation time for the mode of wave vector $\vec{K}$ and N the total number of vortices in the superconducting film. The last term in equation (26) is the purely inductive contribution to $\underset{\sim}{\overrightarrow{\delta E}}_\omega(\vec{q}, z)$ associated with the Meissner response of the superconducting film to the rf-excitation. For weak magnetic fields this term is independent of B and, consequently, it does not contribute to the $\partial V/\partial B$-signal measured in our experiments. Notice that, using equation (24), $\underset{\sim}{\overrightarrow{\delta E}}_\omega(\vec{q}, z)$ can alternatively be expressed in terms of $\underset{\sim}{\vec{j}}_{a\omega}(\vec{q}, q_z = -iq)$ rather than of $\underset{\sim}{\vec{J}}_{M\omega}(\vec{q})$.

In the following we shall discuss the rf-response of the 2D vortex crystal in the different phases it can assume on the periodic substrate.

A. *The commensurate* (C) *phase*

With the vortex crystal in a C-phase, the eigenvectors $\vec{\Phi}_{\mathbf{K}}(\vec{r}_{je})$ appearing in equation (27) are given by equation (7) and, moreover, the $\{\vec{r}_{je}\}$ form a set of lattice vectors. Then, from equation (27) it immediately follows:

$$R_{\omega\alpha\beta}(\vec{q}', \vec{q}) = R_\square(\hat{q}\times\hat{z})_\alpha \sum_{\mathbf{K}} \frac{i\omega\tau(\vec{K})}{1+i\omega\tau(\vec{K})}$$
$$\times[\hat{q}\cdot\hat{e}_t(\vec{K})][\hat{z}\times\hat{e}_t(\vec{K})]_\beta \Delta(\vec{K}-\vec{q})\,\Delta(\vec{K}-\vec{q}'), \quad (28)$$

where the Peierls symbol $\Delta(\vec{p})$ is such that $\Delta(\vec{p}) = 1$ if $\vec{p} = \vec{g}_{mn}$ and vanishes otherwise. From equation (28) it is readily seen that only U-processes contribute to the sum over $\vec{K}$, the scalar product in equation (28) vanishing for $\vec{K} = \vec{q}$. Their contribution to the rf-voltage V, however, is vanishingly small, since, as it follows by considering the exponential factor e^{-qh_R} (where $h_R \gg a$) resulting from the integration of equation (26) over the turns of the receive coil R, the relevant $\vec{q}$-vectors of our experiments are such that $qh_R < 1$ and are therefore confined to the first Brillouin zone ($qa \ll 1$). Thus, we can conclude that $\partial V/\partial B \simeq 0$ for an infinite ideal vortex crystal in a C-phase.

B. *The incommensurate* (I) *phase – Size effects*

In an I-phase the eigenvectors $\vec{\Phi}_{\mathbf{K}}$ are given by equation (9). Moreover, $\vec{r}_{je}$ can be written in the form $\vec{r}_{je} = \vec{r}_{j0} + \vec{w}_{je}$, where $\vec{r}_{j0}$ is a lattice vector of the undistorted triangular vortex lattice and $\vec{w}_{je}$ is the periodic [period $P(\delta)$] transverse ($\vec{w}_{je} \cdot \vec{K} = 0$) deformation field associated with the static 1D soliton superlattice. If one assumes that $\vec{w}_{je}$ varies slowly with the position of the vortex j, the sums over j and l in equation (27) can be replaced by integrals over a smooth density of lattice points. Then, a straightforward calculation leads to the following expression for the vortex response function:

$$R_{\omega\alpha\beta}(\vec{q}', \vec{q}) = R_{\square}(\hat{q} \times \hat{z})_\alpha \sum_{\mathbf{K}} \frac{i\omega\tau(\vec{K})}{1 + i\omega\tau(\vec{K})} [\hat{q} \cdot \hat{e}_t(\vec{K})][\hat{z} \times \hat{e}_t(\vec{K})]_\beta$$
$$\times \sum_{\vec{G},\vec{G}'} \vec{\Psi}_{\mathbf{K}}(\vec{G}) \vec{\Psi}^*_{\mathbf{K}}(\vec{G}')\, \delta_{\mathbf{K},\mathbf{q}-\mathbf{G}}\, \delta_{\mathbf{K},\mathbf{q}'-\mathbf{G}'}, \tag{29}$$

where $\vec{\Psi}_{\mathbf{K}}(\vec{G})$ is the $\vec{G}$-Fourier component of the 'wave function' $\vec{\Psi}_{\mathbf{K}}(u)$, of period P, appearing in equation (9). In our granular Al-films the correlation length R_c sets an upper limit to P ($P \leqslant L \simeq R_c$) which is therefore expected to be much less than h_R ($P \ll h_R$). Since, as shown in the previous subsection, only long-wavelength Fourier components, such that $qh_R < 1$, are important in our experiments, it follows that the relevant $\vec{q}$-vectors are confined within the first Brillouin zone of the 1D soliton superlattice ($qP \ll 1$). Then, by considering the sum over $\vec{K}$ in equation (29), it is readily seen that only U-processes in the reciprocal soliton lattice, such that $\vec{K} = \vec{q} - \vec{G}$ and $\vec{K} = \vec{q}' - \vec{G}'$, contribute to $R_{\omega\alpha\beta}(\vec{q}', \vec{q})$. Furthermore, since $qP \ll 1$ and, consequently, $q \ll G$ and $q' \ll G'$ for the U-processes of interest here, we can set $\vec{K} = \vec{G}$ in equation (29), an approximation which, in turn, implies $\vec{q} \simeq \vec{q}'$. Substituting the resulting diagonal vortex response function into equation (26) and integrating $\overline{\delta\vec{E}_\omega}(\vec{r}, z)$ over the turns of the receive coil R, the rf-voltage V can be written in the form:

$$V_\omega = C(T) Z'(\omega, B, T) I_{a\omega}. \tag{30}$$

In this expression the 'impedance' $Z'(\omega, B, T)$ contains the vortex dynamics and is given by:

$$Z'(\omega, B, T) = R_{\square} \sum_{\vec{G}}{}' \langle \Phi_{\mathbf{G}}(u) \rangle^2 \frac{i\omega\tau(\vec{G})}{1 + i\omega\tau(\vec{G})}. \tag{31}$$

where the sum is over all $\vec{G}$ excluding the $\vec{G} = 0$-mode and the average of $\Phi_{\mathbf{G}}(u)$, which is given by equation (16) for a piece-wise parabolic potential $U(\phi_e)$, is taken over one period P of the soliton lattice. It is easily verified that only those solutions, $k_{\mathbf{G}}$, of equation (15) which correspond to an even standing wave, i.e. to points like A in Fig. 6, lead to a non-vanishing average of $\Phi_{\mathbf{G}}(u)$.

The temperature dependent factor $C(T)$ describes the geometry of the drive and receive coils as well as their orientation with respect to $\vec{q}_0$. If one assumes a unidirectional Meissner sheet supercurrent density of the form $\vec{J}_{M\omega}(\vec{q}) = \hat{D}\chi_D(\vec{q}) I_{a\omega}$ [see Section II, Fig. 1 and equation (24)], $C(T)$ can be written as:

$$C(T) = \int d^2q \frac{e^{-qh_R}}{1 + q\Lambda(T)} \chi_D(\vec{q}) \chi_R(\vec{q}) \Gamma(\hat{q}), \tag{32}$$

where $\chi_D(\vec{q})$ and $\chi_R(\vec{q})$ are 'circuit functions' depending on the geometrical properties of the drive and receive coils respectively. The factor $\Gamma(\hat{q})$ is given by $\Gamma(\hat{q}) = (\hat{q} \cdot \hat{e}_t)[\hat{e}_t \cdot (\hat{z} \times \hat{D})][\hat{q} \cdot (\hat{z} \times \hat{R})]$ and therefore describes the angular dependence of the vortex response [$\hat{e}_t$ is perpendicular to the direction u of the 1D soliton lattice (Fig. 1)]. It should be noticed that current continuity requires $\vec{q} \cdot \underset{\sim}{\vec{J}}_{M\omega}(\vec{q}) = 0$, a condition implying that $\hat{q} \cdot \hat{D} = 0$ for the nearly unidirectional $\vec{J}_M$ of our experiments.

Before proceeding to a qualitative analysis of the experimental data of Section II in terms of the theoretical model studied in Sections III and IV, we recall that the results of this subsection can be applied to a sample of finite size L provided one replaces P by L when the vortex lattice in in a C-phase with boundary solitons (Fig. 7). As shown in Section III(C), in granular films L is of the order of R_c, the Larkin-Ovchinnikov correlation length [21].

C. *Comparisons with experiment and discussion*

Let us first discuss the magnetic field and temperature dependence of the structures observed in $\partial V/\partial B$ about B_{10}. In this connection we notice that $q\Lambda(T) \ll 1$ for the temperatures and q-values ($qh_R < 1$) of interest here and, consequently, $C(T)$ [equation (32)] becomes independent of temperature. {$C(T)$ depends on T only in a narrow temperature range close to T_c, where $\Lambda(T)$ diverges and, as a consequence, $C(T)$ tends to zero as $[1-(T/T_c)]$}. Then, as shown by equation (30), the dependence of the rf-signals on B and T can be simply deduced from numerical calculations of the vortex impedance Z' [equation (31)]. Three parameters enter such calculations: the 'sample size' L, the ratio $\Delta/\mu = (\pi\varepsilon/2q_0)^2$ [24] and the relaxation time $\tau_\Delta = \eta/q_0^2\Delta$ associated with overdamped vortex motion in the periodic pinning potential. Thermal fluctuations of the vortices are roughly taken into account by replacing Δ with $\Delta_R(T)$, the 'renormalized' strength of the pinning potential calculated in Ref. 7 using a self-consistent harmonic approximation. Theoretical field derivatives of the normalized impedance $z' = Z'/R_\square$, as deduced from equation (31) using equation (16) for $\Phi_G(u)$, equation (15) for k_G, equation (11) for $P[\delta(B)]$ and equation (14) for $\tau(\vec{G}) = \eta/E(\vec{G})$, are shown in Fig. 8 for a typical domain size ($L = R_c = 30\lambda_0$) and for values of Δ_R/μ and $\omega\tau_{\Delta R}$ corresponding to three different temperatures. Comparison with the data in Fig. 2 shows good qualitative agreement for the field dependence as well as for the relative magnitude of the real and imaginary parts of the $\partial V/\partial B$-signal. As observed experimentally, the model correctly predicts, for rising temperatures, a gradual decrease of the structures around B_{10} followed by a rapid degradation when T approaches the 'locking-unlocking' temperature T_{LU} [7], above which the vortex lattice no longer feels the periodic pinning structure [$\Delta_R(T_{LU}) = 0$]. At very low temperatures ($T \to 0$), Δ_R/μ and $\omega\tau_{\Delta R}$ become independent of T and, as a consequence, the structures in $\partial V/\partial B$ reach their maximum amplitude. This is in striking contrast with the complete absence of structures in the rf-data taken at temperatures below ~ 1.7 K. This behaviour might be due to the growing (relative) importance of random pinning effects with decreasing temperatures. Further work is needed, however, in order to assess the validity of this conjecture.

To discuss the low-temperature angular dependence of the rf-signals (Fig. 4), we must consider the $\Gamma(\hat{q})$-factor in equation (32). In this connection, we first

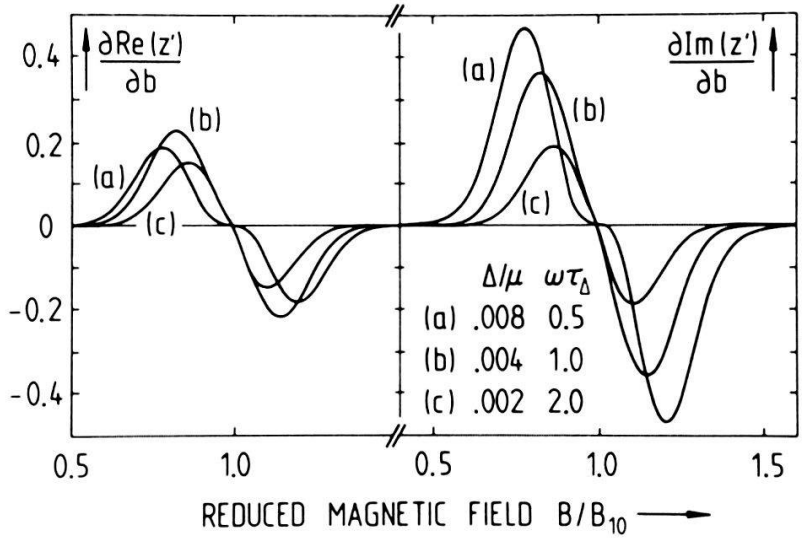

Figure 8
Theoretical field derivatives of the normalized vortex impedance $z' = Z'/R_{\square}$ calculated from equation (31) for three different temperatures. b is the reduced magnetic field B/B_{10}.

notice that all the experimental data presented in this paper were obtained with a drive-receive coil configuration such that $\hat{D}//\hat{R}$ (Fig. 1). As discussed in Section III(C), in granular Al-films the vortex lattice is expected to break up into a large number of uncorrelated domains. For the sake of illustration, we first consider the rather unlikely situation in which the soliton lattice is supposed to have the same orientation, say at +45° with respect to $\vec{q}_0$ (the u-direction in Fig. 1), in all domains. In this case $\Gamma(\hat{q})$ has the same value for both the (x, x)- and the (y, y)-configurations: $\Gamma_{xx} = \Gamma_{yy} = 1/2$. For the $(x+y, x+y)$-configuration we distinguish two cases: (i) $\hat{D}$ (and $\hat{R}$) parallel to the soliton lattice, for which $\Gamma_{x+y,x+y} = 1$ and (ii) $\hat{D}$ (and $\hat{R}$) perpendicular to the soliton lattice, for which $\Gamma_{x+y,x+y} = 0$. This strongly anisotropic behaviour of the low-temperature dynamic vortex response was not observed in our experiments. On the other hand, if one assumes that the vortex crystal breaks up into uncorrelated domains in which the orientation of the solitons randomly changes from +45° to −45° with respect to $\vec{q}_0$, a simple averaging procedure, which assumes an equal number of domains for the two possible orientations, leads to $\langle\Gamma(\hat{q})\rangle = \Gamma_{xx} = \Gamma_{yy} = \Gamma_{x+y,x+y} = 1/2$. This reasonably agrees with the nearly isotropic rf-response observed at low temperatures (Fig. 4), a result providing convincing evidence for a multidomain structure with solitons randomly oriented at ±45° with respect to the thickness modulation.

At high temperatures, where a new strongly anisotropic signal shows up in the rf-data (Figs. 3 and 5), our model fails in describing the dynamic vortex response. This might be due to the formation of liquid-like domains in a temperature range which is above the 2D melting temperature [9–11]. Calculations of the dynamic response in such a régime will be done in the near future.

Acknowledgements

We would like to thank J. R. Clem and V. L. Pokrovsky for many stimulating discussions. This work has been supported by the Swiss National Science Foundation.

REFERENCES

[1] P. Bak, Prog. Phys. *45*, 587 (1982).
[2] O. Daldini, P. Martinoli, J. L. Olsen and G. Berner, Phys. Rev. Lett. *32*, 218 (1974).
[3] P. Martinoli, O. Daldini, Ch. Leemann and E. Stocker, Solid State Commun. *17*, 205 (1975).
[4] P. Martinoli, O. Daldini, Ch. Leemann and B. Van den Brandt, Phys. Rev. Lett. *36*, 382 (1976).
[5] P. Martinoli, Phys. Rev. B *17*, 1175 (1978).
[6] P. Martinoli, H. Beck, M. Nsabimana and G. A. Racine, Physica *107B*, 455 (1981).
[7] P. Martinoli, M. Nsabimana, C. A. Racine, H. Beck and J. R. Clem. Helv. Phys. Acta *55*, 655 (1982).
[8] V. L. Pokrovsky and A. L. Talapov, Phys. Rev. Lett. *42*, 65 (1979); Sov. Phys. JETP *51*, 134 (1980).
[9] J. M. Kosterlitz and D. J. Thouless, J. Phys. C *6*, 1181 (1973).
[10] B. A. Huberman and S. Doniach, Phys. Rev. Lett. *43*, 950 (1979).
[11] D. R. Nelson and B. I. Halperin, Phys. Rev. B *19*, 2457 (1979).
[12] A. T. Fiory, Phys. Rev. B *8*, 5039 (1973).
[13] A. T. Fiory and A. F. Hebard, AIP Conf. Proc. *58*, 293 (1980).
[14] J. R. Clem, private communication.
[15] L. Landau and E. Lifshitz, *Theory of elasticity* (Pergamon Press, London, 1970), Ch. III.
[16] J. Bardeen and M. J. Stephen, Phys. Rev. *140A*, 1197 (1965).
[17] S. E. Burkov and V. L. Pokrovsky, J. Low Temp. *44*, 423 (1981).
[18] F. Patthey, M. S.-Thesis (Université de Neuchâtel, 1984), unpublished.
[19] S. Flügge, *Rechenmethoden der Quantentheorie* (Springer-Verlag, Berlin, 1965), p. 59.
[20] P. A. Lee, T. M. Rice and P. W. Anderson, Solid State Commun. *14*, 703 (1974).
[21] A. I. Larkin and Yu. N. Ovchinnikov, J. Low Temp. Phys. *34*, 409 (1979).
[22] P. H. Kes and C. C. Tsuei, Phys. Rev. B *28*, 5126 (1982).
[23] J. Pearl, PhD-Thesis (Polytechnic Institute of Brooklyn, New York, 1965), unpublished.
[24] As shown in Ref. 7, Δ/μ is of the order of $4(\Delta d/d)$.